

PCCP

Accepted Manuscript



This is an *Accepted Manuscript*, which has been through the Royal Society of Chemistry peer review process and has been accepted for publication.

Accepted Manuscripts are published online shortly after acceptance, before technical editing, formatting and proof reading. Using this free service, authors can make their results available to the community, in citable form, before we publish the edited article. We will replace this *Accepted Manuscript* with the edited and formatted *Advance Article* as soon as it is available.

You can find more information about *Accepted Manuscripts* in the [Information for Authors](#).

Please note that technical editing may introduce minor changes to the text and/or graphics, which may alter content. The journal's standard [Terms & Conditions](#) and the [Ethical guidelines](#) still apply. In no event shall the Royal Society of Chemistry be held responsible for any errors or omissions in this *Accepted Manuscript* or any consequences arising from the use of any information it contains.

ARTICLE

New Molecular-Scale Information of Polystyrene Dynamics in PS and PS-BaTiO₃ composites from FTIR spectroscopy

Cite this: DOI: 10.1039/x0xx00000x

D. Olmos,^a E. V. Martín^a and J. González-Benito^{a*}Received 00th January 2012,
Accepted 00th January 2012

DOI: 10.1039/x0xx00000x

www.rsc.org/

A new idea to understand the macromolecular motion occurring along the thermal relaxations of polystyrene (PS) and PS-barium titanate composites is proposed. Detailed analysis of PS infrared bands provides a better knowledge of the factors affecting polymer dynamics. Average spectral positions and integrated absorbance of bands in the region of C-H out-of-plane vibrations showed a continuous decrease with temperature, whereas those in the region of aliphatic and aromatic C-H stretching vibrations showed the sharpest changes with temperature. Relaxation temperatures were determined from the changes observed in the bands wavenumber or area with temperature. These results were attributed to changes in the distribution of the phenyl π -electron cloud, causing important dipole moment variations in the different vibration modes when the thermal transitions are taking place. Finally, although the presence of BaTiO₃ particles does not seem to exert any specific effect on the PS dynamics in the glassy state, the Curie transition of these particles might induce a kind of confinement effect observable by FTIR.

1. Introduction

It is well-known that addition of ceramic nanoparticles to polymers allows obtaining materials with improved or unique properties (electrical, magnetic, optical, mechanical...). Among other things, particle size and dispersion are critical in modifying properties of composites [1-4]. Besides, uniform particle dispersion should ease the task of interpreting data about the effect of particles in the properties of a polymer. For this reason, many attempts were done to distribute particles uniformly within a polymer matrix. In general, when the ratio between the amount and size of particles is too high, a uniform dispersion of them is rarely achieved. Recently, using high energy ball milling (HEBM) it was possible to prepare materials with an efficient dispersion of nanoparticles within different thermoplastic polymers [5-10].

In particular, much about the effect of particles on polymer dynamics is not well understood yet. For example, some studies suggest that the presence of nanoparticles, can lead to specific chain conformations that would yield, as a result, modified properties in polymers [7]. Other works point out that specific interactions between the particles and the polymer restrain the macromolecular chain motion at the interface [11]. However, up to the present moment no clear information coming from experimental results about the local origin of polymer chain dynamics is given.

In polymer science, knowledge of macromolecular chain dynamics (i.e., how and why they move) is one of the most important issues to understand polymer properties. For instance, to know if particular motions of a group or groups of atoms are the main driving forces of the polymer dynamics could be the starting point. In this sense, instruments capable of extracting information at a local scale are essential to carry out these studies.

Due to the important changes in polymer dynamics, one of the most important parameters for materials design is the temperature or temperature range of any thermal transition, such as the glass transition temperature (T_g). In the case of composites, depending on the inter-particle distances, the strength of the polymer-filler interactions and confinement effects different scenarios are possible: i) a decrease in T_g [12] (as free volume increases, the chain segment mobility near the particles increases too); ii) an increase of T_g [13, 14] (the polymer-particle interactions slow down the chains motion); iii) no impact on the dynamics of polymer chains [15]. Therefore, to prepare tailor-made materials it is very important to understand the influence of the processing and the presence of filler on the structural changes and dynamics of polymers.

Fourier transform infrared (FTIR) spectroscopy is a very selective analytical technique useful for investigating the conformation, inter and intra-molecular interactions in polymers [16]. Under thermally controlled conditions FTIR

spectroscopy has been used to study the chemical reactivity and physical properties of polymers at a molecular level [17]. For example, in polymer synthesis or degradation, FTIR enables us to monitor as a function of temperature and time changes in the polymer structure. Thus, kinetic studies of chemical reactions can be done following variations in chemical composition (functional groups appearance or disappearance) from the appearance and/or disappearance of certain absorption bands [18-21]. Other studies include polymer crystallization [22-24]; phase and molecular transitions in polymers [17]; conformational changes [7]; vibrational relaxation of tactic polymers [25, 26]; physical aging [27] and phase separation processes in polymer blends [28]. To our knowledge, none of these works deals with an in-depth analysis where most absorbing bands in the spectra had been considered. The most general approach only takes a few IR absorption bands representative of most molecular groups or bond vibrations. However, this is not usually enough to have a real vision about the movement of the polymer chain in different molecular sites. Therefore, in this work is suggested to correlate the dynamical state of the polymer with most IR active motions of the different molecular groups (most of the observed IR bands).

In polymer spectroscopy, the study of bands shapes and widths [7, 25] is a common practice since they are related with the distribution of the different local environments experienced by the absorbing or emitting groups. In general, for any given absorption or emission, bands usually reflect the superimposition of different frequencies resulting from the interactions in slightly different local environments [7, 25, 29-31]. In this work, it is proposed, in a very simple way, the use of FTIR spectroscopy to understand the changes that take place along the dynamical behavior of polystyrene (PS) with temperature. Besides, using this kind of information, the effect that the presence of sub-micrometric BaTiO₃ particles may exert on glass transition of the polymer will be more accurately interpreted. Band shifts ($\langle \nu \rangle$, cm⁻¹) and absorbance variations with temperature will be analyzed to study the induced structural changes and polystyrene dynamics. Finally, the effect BaTiO₃ sub-micrometric particles in structural changes of PS will also be considered.

2. Experimental

2.1. Materials. Pellets of atactic polystyrene supplied by Sigma Aldrich (CAS 9003-56-6) was used in this study (PS, Mw ≈ 192000; melt index 6.00 – 9.00 g/10min 200°C/5.0 kg, ASTM D 1238 and softening point 107°C, Vicat, ASTM D 1525). Barium titanate submicrometric particles (BaTiO₃, 200 nm of diameter) were purchased by Nanostructured and Amorphous materials Inc (99.9% purity, density 6.02 g/cm³ and tetragonal crystalline structure checked by X-ray diffraction).

2.2. Sample preparation. Mixtures of PS and BaTiO₃ particles with different compositions (0%, 1%, 2%, 4% and 10%, weight percentages) were prepared by cryo-milling using a MM400 RETSCH miller machine. A stainless steel vessel of 50mL of capacity and one ball of 25-mm diameter were used. The process was carried out as follows: 1h of active cryomilling divided into 12 milling cycles of 5min at 25Hz and 15 min of resting in liquid nitrogen. Following this protocol cross-contamination of iron can be considered negligible since in the samples with 10% wt of particles, less amount of Fe than 0.003% was detected [32].

2.3. Materials characterization. Structural characterization was performed by Fourier transformed infrared spectroscopy, FTIR, using a FT-IR Spectrum GX (Perkin-Elmer). The spectra were recorded at a constant temperature from 400 to 4000 cm⁻¹ by averaging 5 scans at a resolution of 4 cm⁻¹. The powders coming from the cryomilling process were diluted in KBr (3% wt/wt), mixed homogeneously using an Agatha mortar and then pressed uniaxially at 2 Tons for 5 minutes to subsequently prepare the samples in the form of disks. The samples were then studied in the transmission mode by FTIR.

2.4. Study of thermal transitions in PS. To eliminate thermal and processing histories (residual stresses given by the shear forces exerted by the milling for instance), the samples were heated at 150 °C for 60 minutes in an oven and then quenched to room temperature. After that, to study thermal transitions transmission FTIR spectra of the samples were recorded along a thermal ramp from 35 °C – 160 °C at 2.5°C/min. The samples were introduced in an commercial sample holder suitable for temperature dependent experiments from SPECAC and the temperature ramp was controlled with a home-made program. The heating rate was chosen to match with the acquisition time of the FTIR spectra. The experiments are done using a constant nitrogen flow to avoid oxidation of the samples during the experiment.

2.5. Data analysis. The position of the absorbance peaks is considered to account for a distribution of spectral contributions. Owing to the small changes that occur in the band, the position of the band was evaluated through the frequency first moment expressed as follows (eq.1):

$$\langle \nu \rangle (\text{cm}^{-1}) = \frac{\sum_{\text{band}} A(\nu_i) \cdot \nu_i}{\sum_{\text{band}} A(\nu_i)} \quad (1)$$

where A(ν_i) is the absorbance at each frequency (ν_i) within a given absorption band. Since $\langle \nu \rangle$ is a mean vibrational frequency of a certain oscillator affected by different environments, it should provide useful information about the different conformational contributions. Therefore, in the case of polymers, this parameter will account for a weighted average of all the different environments affecting the changes observed in a specific bond vibration caused by its most immediate surroundings. Depending on the different kinds of specific interactions of the functional groups the environment of the bond may vary and so its average frequency $\langle \nu \rangle$.

The integrated absorbance is the band area that can be expressed by the equation (2). Again, A(ν_i) is the absorbance at each frequency (ν_i) for the absorption band considered.

$$\text{Area} (AU \cdot \text{cm}^{-1}) = \sum_{\text{band}} A(\nu_i) \quad (2)$$

3. Results and discussion

Figure 1 shows the infrared spectrum between 3400-400 cm⁻¹ of the neat polystyrene under study. The band positions and assignments are given in the Table 1 [33-36]. Since the spectrum was obtained dispersing small particles of milled PS in KBr, the scattering phenomena were slightly higher than in those spectra obtained from cast films. However, the spectra are susceptible of being baseline corrected giving typical PS

spectra that only show the small variations that will be commented throughout this article.

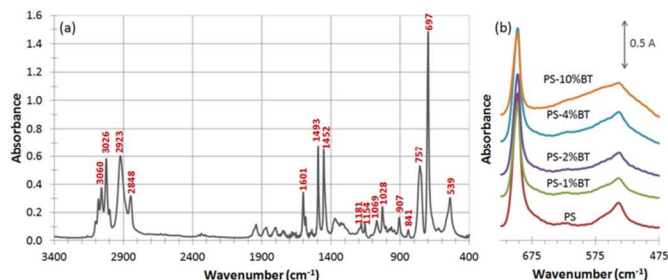


Fig. 1. (a) Infrared spectrum of milled polystyrene at room temperature. The numbers show the peak positions of the main absorption bands analyzed in this work. (b) Low energy range for the spectra of the composites with different content of BaTiO₃ (BT) particles.

The part of the spectrum ranging from 3200 to 2800 cm⁻¹ represents the region of the C-H stretching modes. The peaks at 3082, 3060 and 3026 cm⁻¹ correspond to absorptions from the aromatic C-H stretching vibrations, while the absorption bands at 2923 and 2848 cm⁻¹ come respectively from the asymmetric and symmetric stretching vibrations of methylene groups -CH₂. The pattern of the overtone and combination bands in the region 2000-1665 cm⁻¹ reflects what was expected for mono-substituted aromatic rings (1947cm⁻¹; 1889 cm⁻¹; 1807 cm⁻¹; 1749 cm⁻¹ and 1668 cm⁻¹). The carbon-carbon stretches in the aromatic ring are observed at 1601 and 1583 cm⁻¹ and both represent in-plane ring breathing modes [25]. The absorptions at 1493 cm⁻¹ and 1452 cm⁻¹ are also due to carbon-carbon stretching vibrations in the aromatic ring. However, the band at 1452 cm⁻¹ may result from both the ring breathing of the benzene ring, ν_{19B} (B₁), and the deformation vibration of -CH₂ [34]. The intermediate part of the spectrum, from 1300 cm⁻¹ to 900 cm⁻¹ approximately, is usually referred to as the fingerprint region. In-plane bending bands appear in this region, although these bands are usually very weak in most aromatic compounds. The in-plane C-H bending of the phenyl ring are observed at 1069 and 1028 cm⁻¹. The pattern of the out-of-plane (oop) C-H bending bands in the region 900-675 cm⁻¹ is also characteristic of the aromatic substitution pattern, being intense at 697 and 757 cm⁻¹ respectively. The main absorption peaks of PS are also present in the composites under study. The most remarkable effect is the increase of absorbance and broadening of the band centered at 550cm⁻¹ due to the Ti-O vibration as the content of BaTiO₃ increases (Figure 1(b)).

Most of the previous works have studied polymers relaxation phenomena from an abrupt change in FTIR peaks intensity when it is represented as a function of temperature [37-39]; however, other methods have been investigated. For example, after fitting a particular band to Gaussian or Lorentzian profiles P. Painter et al used the half-width variations to study thermal transitions of PS [25]. More recently, Liang and Huang [27] proposed the use of the FTIR band area to study the glass transition and the physical aging of PS. P. Papadopoulos et al [40] used vibration frequency shifts and integrated band absorbance of some bands to study thermal transitions in PS. As new way to study the thermal relaxation phenomena and determine the glass transition temperature in polystyrene, in this work, the use of the first moment of the absorption band,

$\langle \nu \rangle$ (eq. (1)), is proposed to indirectly increase the accuracy for bands shifts monitoring [41]. Additionally, the integrated band area, A (eq (2)), was used to reinforce the interpretation of macromolecular dynamics of PS.

Table 1. Observed absorption bands for polystyrene. Band assignment and band short-cut name used in this work [33-36].

Frequency (cm ⁻¹)	Intensity	Band assignment	Type
3083	mw	ν_{20B} (B ₁)	
3061	ms	ν'_{20A} (A ₁)	
3026	s	ν'_2 (A ₁)	
2923	s	-CH ₂ stretching	asymmetric III
2848	ms	-CH ₂ stretching	symmetric
Aromatic combination bands in mono-substituted rings.			
	mw	$\nu_{17A} + \nu_5 = 1947$ (B ₁) $\nu_{17B} + \nu_5 = 1889$ (A ₁) $\nu_{10A} + \nu_{17A} = 1807$ (A ₁) $\nu_{10A} + \nu_{17B} = 1749$ (B ₁) $\nu_{10B} + \nu_{17B} = 1668$ (A ₁)	
1601	ms	ν_{9B} (B ₁) = 1602	
1583	w	ν_{9A} (A ₁) = 1585	
1542	vw	$\nu_{11} + \nu_{10A}$	II
1493	s	ν_{19} (A ₁)	
1452	s	δ (CH ₂); ν_{19B} (B ₁)	
1374	m	ν_{14B} (B ₁)	
1328		$1328 = \nu'_3$ (B ₁)	
1310	w	$1310 = \nu_{14B}$ (B ₁)	
		γ_t (CH ₂)	
1181	w	ν (C-C)	
1154		ν'_{15} (B ₁)	
1069		ν'_{18B} (B ₁)	
1028		ν_{18A} (A ₁)	
907	m	ν_{17} (B ₂) 907 cm ⁻¹ band in <i>a</i> -PS is a localized (conformationally insensitive) out-of-plane bending mode of the hydrogen atoms on the phenyl ring.	I
841		ν_{10} (A ₂) (Amorphous PS)	
757	vs	ν_{10B} (B ₂)	
697	vs	ν_{11} (B ₂)	
620	vw	ν_{6B} (B ₁)	
560			
540	s	ν_4 (B ₂)	

s: strong; ms: medium strong; w: weak, mw: medium weak, m: medium, vs: very strong, vw: very weak.

The use of the first moment of spectral bands allows following very small spectral shifts with an indirectly increased accuracy, thus avoiding the limitations imposed by the measurement resolution of the equipment [41]. Furthermore, while former

works have focused on the study of a few bands of the IR spectra, here a full analysis of the evolution of many observable bands is provided. In this way, it is possible to identify what are the most sensitive bands to monitor thermal transitions in PS, allowing us to extract the clearest information relative to conformational changes occurring in polymer chains. The study of thermal transitions is first discussed in terms of the first moment of the absorption bands ($\langle\nu\rangle$) and then in terms of the bands area.

Based on the dependence of the spectral parameters with temperature three spectral regions were identified: region I, II and III. Bands in the region I ($\sim 400\text{--}900\text{ cm}^{-1}$) correspond to the out-of-plane vibrations of the C-H bend of the aromatic ring. The region II ($\sim 900\text{--}2000\text{ cm}^{-1}$) hosts the ring breathing modes and in-plane C-H deformations while, in the region III ($\sim 2800\text{--}3200\text{ cm}^{-1}$) the aliphatic and aromatic C-H stretching vibrations are considered.

Region I. Bands which may change slightly in frequency or absorbance are those appearing in the lowest energy region of the spectrum. As an example, in Figure 2, the variation of the first moment ($\langle\nu\rangle$) of the absorption band centered at 700 cm^{-1} is shown. Similar results were obtained for the peaks centered at 539 , 757 , 840 and 907 cm^{-1} (Electronic Supporting Information, Fig. S1).

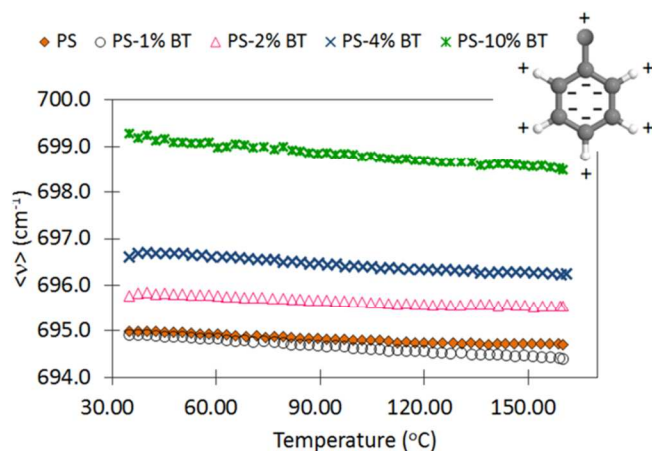


Fig. 2. Evolution of $\langle\nu\rangle$ (cm^{-1}) vs temperature ($^{\circ}\text{C}$) for the bands centered at 700 cm^{-1} . The inset shows a schematic representation of the phenyl ring deformations associated with the vibration mode. The plus and minus signs indicate the two opposite directions of the out of plane vibrations. The color code shows the content in BaTiO₃ particles. (Electronic Supporting Information, Fig. S1).

These bands exhibit a continuous decrease of $\langle\nu\rangle$ (cm^{-1}) with temperature. This result may be associated to an increase in the population of the most energetic rotational levels of the corresponding vibrational ground state. This effect is usually called *hot bands* which are red shifted respect to the corresponding fundamental transitions (they appear at lower wavenumbers) [42]. The magnitude of the observed shift is usually correlated to the degree of anharmonicity in the corresponding normal modes. In these representations a clear slope change cannot be distinguished (Figure 2). Consequently, these bands are not adequate to be used for the detection of thermal relaxations as the glass transition of the polymer. To interpret this unexpected behavior it is considered that the

effect of phenyl oligomers (dimers, trimers, etc) disruption is negligible on these vibrational bending modes. At temperatures below the T_g the probability of having phenyl groups inter and intramolecularly interacting by their aromatic electrons is large, so that, the probability of having phenyl aggregates must be high. However, as the temperature increases the probability of disrupting those aggregates must increase as well, finding the highest probability for that to occur at temperatures well above the T_g . For the aromatic bending modes considered here it is not expected a large change in the π electron distribution or a big distortion of the aromatic electronic cloud with or without interactions. Therefore, the disappearance of phenyl aggregates should not considerably affect the energy required to activate those vibrations.

Region II. Bands within this region are characterized by a noticeable change in the slope of the $\langle\nu\rangle$ vs T plots. In Figure 3, the evolution of $\langle\nu\rangle$ with temperature is shown for the bands centered at 1450 , 1493 and 1600 cm^{-1} (Electronic Supporting Information Fig S2 for bands centered at 1028 , 1069 and 1154 cm^{-1}). Again, this continuous decrease of $\langle\nu\rangle$ (cm^{-1}) observed with increasing temperatures may be associated to an increase in the population of more energetic rotational levels. The transition temperatures estimated from bands in this region (II) were close to $120\text{ }^{\circ}\text{C}$.

By dynamic infrared linear dichroism spectroscopy (DIRLD) I. Noda observed for PS a transition point occurring around 125°C that was assigned to the polymer chain backbone dynamics [43]. This interpretation is reasonable since more energy should be necessary to activate more hindered motions as those associated to the polymer chain backbone. Consequently, bands in region II seem to be useful to study the polymer chain backbone dynamics of polystyrene. According to I. Noda, the glass transition temperature observed for PS around $100\text{ }^{\circ}\text{C}$ is mainly dominated by the dynamics of the aromatic side group rather than the polymer chain segmental motions that appear at higher temperatures ($\sim 125\text{ }^{\circ}\text{C}$) [41]. In his research I. Noda suggested that the glass transition of PS determined by conventional techniques does not seem to involve highly coordinated cooperative segmental motions along the polymer chains as previously believed [43]. In this sense, this research helps to clarify this issue. From the analysis of certain bands, FTIR allows easily to obtain the temperature by which those coordinated cooperative segmental motions along the polymer chains may occur. In fact, when the rupture of aromatic ring aggregates takes place above the transition temperature the cooperative motions are more probable. In the region II, bond vibrations lead to a higher variation in the distribution of π electrons. Therefore, the changes caused varying the proximity between aromatic rings (interactions) should have more effect on the corresponding absorption frequency. In this sense, if the presence of interactions usually leads to a decrease in the frequency of the absorption bands then, when the interactions are suppressed, for instance, after disrupting phenyl aggregates, the first moment ($\langle\nu\rangle$, cm^{-1}) should increase, as it is observed for the transition temperatures in the plots of Figure 3.

The slope changes along the thermal transition showed that the least sensitive band was 1028 cm^{-1} while the most abrupt changes were observed when the band at 1450 cm^{-1} is used (Fig. S2 and Fig. 3 respectively). This result may be explained considering a cumulative effect for the band at 1450 cm^{-1} since two molecular vibrations participate, one corresponds to the

breathing mode of the ring and, the other, to the bending of the methylene. Note that even though variations within the temperature range of the thermal transition are small, the overall trend is always the same and behavior is reproduced for every sample. This ability to reproduce such small changes is obtained averaging the band frequencies with the use of the first moment. On the other hand, Figure 3 also shows that none of the vibrations in region II is sensitive to the content of BaTiO₃ particles.

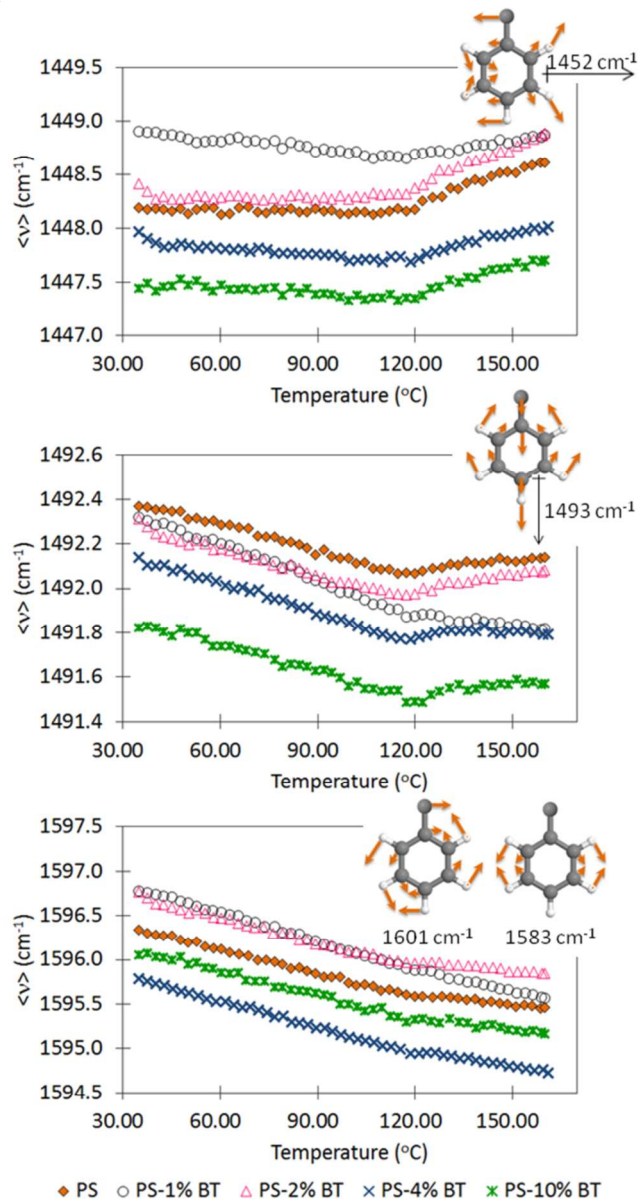


Fig. 3. Evolution of $\langle \nu \rangle$ (cm⁻¹) vs temperature (°C) for the bands centered at 1450, 1493 and 1600 cm⁻¹. The insets in each graph show a schematic representation of the phenyl ring deformations associated with each vibration mode. The arrows indicate the relative motions of the atoms in space. The color code shows the content in BaTiO₃ particles.

Region III. Bands in this region correspond to the aliphatic and aromatic C-H stretching vibrations. To avoid band deconvolution and baseline effects in the analysis, aliphatic C-

H stretching bands were integrated altogether, i.e. the asymmetric and symmetric C-H stretching vibrations were considered to be represented by a single band. The same process was used for the aromatic C-H stretching vibrations. The results obtained for the plots of $\langle \nu \rangle$ vs T are shown in Figure 4.

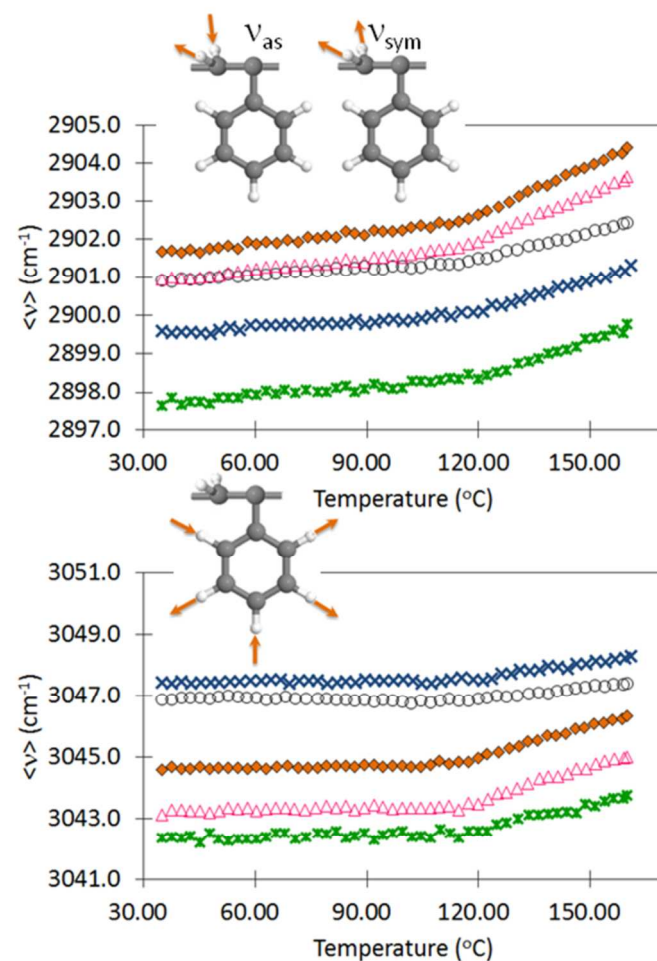


Fig. 4. Evolution of $\langle \nu \rangle$ (cm⁻¹) vs temperature (°C) for the bands corresponding to the aliphatic (top) and aromatic (bottom) C-H stretching vibrations. The insets in each graph show a schematic representation of the vibrations. The arrows show the relative motions of the atoms in space. The color code shows the content in BaTiO₃ particles.

The graphs in Figure 4 show that $\langle \nu \rangle$ increases with temperature. In this case it is also possible to find slope changes which are even sharper than those observed in regions I and II. Therefore, these bands seem to be appropriate to study thermal relaxations as the glass transition of the polymer. The transition temperatures extracted from the graphs were found at approximately 115 °C although the temperatures determined using the aromatic CH stretching vibrations (Figure 4, bottom) were slightly below the ones obtained using the aliphatic CH vibrations (Figure 4, top). The same result was obtained from the band area analysis and so, a more detailed explanation is provided there. Once more, no significant differences with the content of BaTiO₃ particles are observed.

Since several bands were considered altogether, there are two possible explanations to justify the spectral frequency variations observed here: i) either there is a band shift in terms of frequency to higher frequency values or ii) there is a change in the intensity ratio of the bands. A shift to higher frequencies does not seem to be very likely to happen as the temperature increases. In fact, the presence of the *hot bands* would not explain this shift to higher frequencies. One possible explanation is that for the most energetic vibration there is a larger change in the dipole moment when temperature increases. The later can be explained considering an increase in the free volume that provides more space available to favor larger dipole changes. Thus, to discriminate the factor that mainly affects these shift variations; band area analysis will be used.

The study of the polymer dynamics by FTIR was complemented by the analysis of the areas of the absorption bands, as indicated in equation (2), considering the same three regions.

Region I. As an example, in Figure 5, the variation of the band area with temperature is shown for peaks centered 700 cm^{-1} (Similar results were obtained for bands centered at 540 , 757 , 840 and 907 cm^{-1} Supplementary information Fig S3). The general trend in this region is a continuous decrease in band area with temperature. The most common interpretation for this behavior may be in terms of the number of absorbing species. As temperature increases, the material density decreases the concentration of absorbing species decreases and therefore their corresponding optical density. No significant changes in the slope of the plots are observed. Only a small change in the slope of the band centered at 907 cm^{-1} can be seen, whose estimated transition temperature is close to $115\text{ }^{\circ}\text{C}$. Essentially, this means that the least energetic vibrations of PS are not sensitive enough to be used for monitoring thermal transitions in polystyrene.

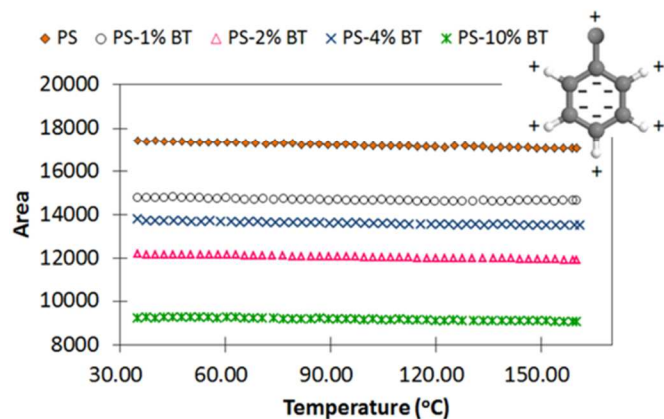


Fig. 5. Evolution of band areas as a function of temperature ($^{\circ}\text{C}$) for the bands centered at 700 cm^{-1} . The inset in each graph show a schematic representation of the phenyl ring deformations associated with each vibration mode. The color code shows the content in BaTiO_3 particles.

Region II. Figure 6 depicts the plots of band area vs temperature for the bands in this spectral range. Since differences in band area were relatively high, only the plots obtained for neat PS are shown for clarity (the rest of plots for all the samples under study show similar profiles).

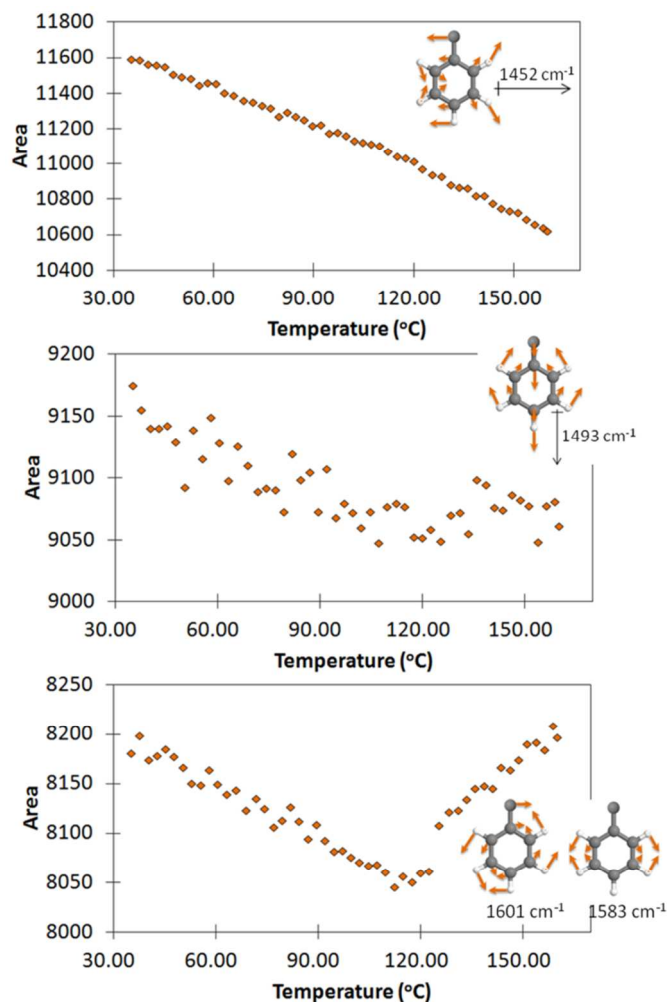


Fig. 6. Temperature dependence of band areas for bands centered at 1450 (top), 1493 (middle) and 1600 cm^{-1} in PS. The insets in each graph show a schematic representation of the phenyl ring deformations associated with each vibration mode (See Supporting Information for bands at 1028 , 1069 and 1154 cm^{-1} , Fig. S4).

The first part of the curves shows a clear decrease of the band area as temperature increases. Again, this dependence is in accordance with a decrease in the concentration of absorbing species associated with the decrease in the density of the polymer. After the T_g , the slope of the curve changes, either remaining constant or slightly increasing with temperature. These differences in the general behavior of the bands considered in this region may be due to different factors. For example, the bands at 1450 and 1600 cm^{-1} are combination of two vibrations.

Although the band at 1450 cm^{-1} is the result of the overlapping of two vibrations at this frequency, it was also possible to determine a thermal transition at 115°C , since a change in the slope was observed at that temperature. It should be noted that despite the contribution of the CH_2 to the band area of the ring breathing mode of benzene, this band could be used to monitor thermal transitions in PS so its analysis was also included here for comparison.

Likewise, the band area of the band centered at 1600 cm^{-1} results from the combination of the two in-plane ring breathing modes at 1601 and 1583 cm^{-1} respectively [25]. To avoid curve fitting from a deconvolution, the two bands were analyzed together as a whole. Since frequencies are very close, absorbance band ratio (A_{1601}/A_{1583}) was calculated to separate the effects due to the different vibrations (Figure 7). Though a transition is observed, the change in the slope is less sharp than in the case of the plot shown in Figure 6 (bottom). Therefore, band ratio analysis did not seem to be the best choice for this study about thermal transitions. P. Painter et al [25] did an exhaustive work on the study of all the effects and factors affecting the C-C bond vibrations. In fact, P. Painter et al [25], using the half band width to study thermal transitions of PS, found it necessary to take into account two additional bands (not visible in the spectra), at 1593 and 1577 cm^{-1} , in order to obtain a good fit of the two absorption bands. To avoid assuming the appearance of two additional bands, in this study it is proposed to follow the variation of these bands as seen in the spectra.

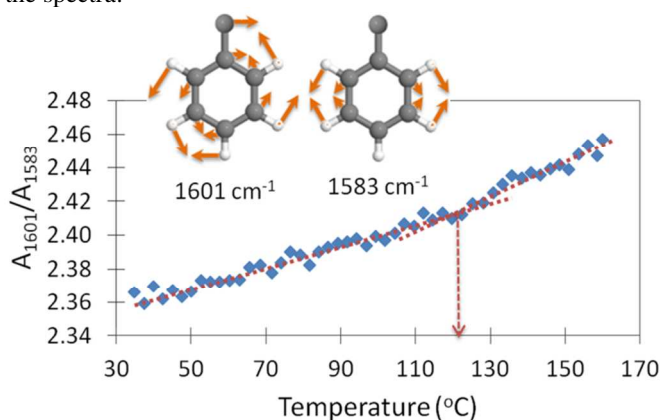


Fig. 7. Temperature dependence of absorbance band ratio (A_{1601}/A_{1583}) for PS. The dashed lines show the best linear fittings from whose intersection the transition temperature is determined.

Except for the bands at 1450 and 1600 cm^{-1} , the plots in Fig. 6 (and Fig. S4) correspond to single non-overlapping vibrations. The band area of the vibration at 1493 cm^{-1} is the one that shows the highest dispersion with temperature. It corresponds to the vibration of the phenyl ring in a position that is perpendicular to the hydrocarbonated chain of the polymer. Yet a transition temperature of approximately 115 °C was also determined. A similar behavior was found for the band at 1028 cm^{-1} . The band area of the vibration at 1154 cm^{-1} did not show any significant change either with temperature or with the content of BaTiO_3 particles.

According to X. Liang [27] two opposite effects may influence the intensity of an IR band insensitive to the temperature. On the one hand, when heating the sample the free volume increases, reducing the density of the sample. As a result, the IR absorption per unit volume of the sample decreases, leading to a reduction in band intensity [37]. On the other hand, when the free volume is increased more space for the segmental motions is available resulting in larger changes in the dipole moment, which should increase the band intensity [44]. The different balance between these two factors in the studied vibrations might explain the absorbance variations observed here.

Region III. In Figure 8, the evolution of the band area with temperature for the bands associated to the aliphatic and aromatic C-H stretching vibrations of PS is shown. The insets (in Figures 8(a) 8(b)) illustrate the small variations in absorbance observed in the bands used to obtain band area.

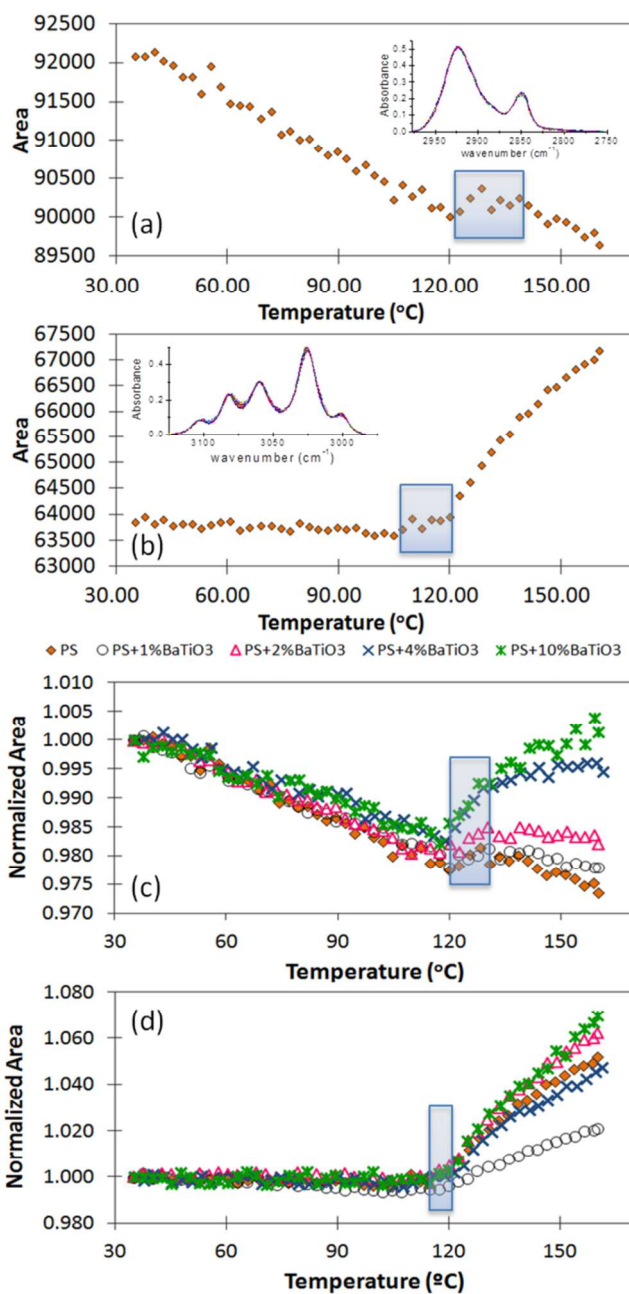


Fig. 8. Evolution of the band area with temperature for the bands associated to: (a) the aliphatic C-H and (b) the aromatic C-H stretching vibrations of PS. The insets show the spectra used for the integration of these bands. (c) and (d) show the normalized band areas vs temperature of the aliphatic and aromatic CH vibrations respectively for the samples with different content of BaTiO_3 .

Both group of vibrations (aliphatic and aromatic) exhibit a disruption in the initial linear behavior that could be assigned to a thermal transition. The shaded region corresponds to the

range of temperatures wherein this process takes place. It is noteworthy to mention that the transition begins at about 120 °C in the case of the aliphatic C-H vibrations (Figure 8 (a)) whereas the process starts at slightly lower temperatures, around 110 °C approximately, when aromatic C-H vibrations are considered (Figure 8(b)). These effects are also observed when the composites with BaTiO₃ are considered. Figures 8 (c) and (d) include the results of normalized band areas vs temperature of the aliphatic and aromatic CH vibrations for the samples with increasing content of BaTiO₃. The data were normalized to the band areas of the first spectrum at the lowest temperature measured. Figure 8 (c) shows that there is an abrupt change in the slope at about 120 °C for every sample. There are two remarkable facts that must be taken into account when the content of particles is considered: i) the normalized absorbances (i.e. the jump in absorbance) observed after 120 °C are higher the higher the content of particles and ii) the range of temperatures till the second change of slope (see the behavior of pure PS) is larger with the content of particles. This may indicate that BaTiO₃ particles may be somehow interfering in the interactions existing among the macromolecules of polystyrene. A possible explanation is related with Curie transition of the BaTiO₃ particles since, when this transition occurs and increase of particle volume takes place what might exert a kind of confinement effect. In a previous study [31] a different behavior of the intrinsic fluorescence intensity of PS-BaTiO₃ composites than those observed in pure PS at approximately 123 °C was reported. This fact was associated to the expansion of the BaTiO₃ particles as a consequence of Curie transition, changing the stacking of the chains and favoring the multimer formation.

Though not as clearly noticeable as in Figure 8 (c), in Figure 8 (d) it is possible to distinguish that transition temperatures ranged from 110 °C to 120 °C. Here no significant differences were observed with the content of particles, probably because a larger number of bond vibrations are being analyzed and variations may not be as directly perceived as in the case of the aliphatic CHs.

The behavior of band area with temperature however, strongly depends on the bands analyzed. For example, the band area decreases continuously with temperature for the stretching vibrations of the aliphatic C-H (Figure 8(a)). On the other hand, at higher temperatures the band area increases continuously with temperature for the stretching vibrations of the aromatic C-H (Figure 8(b)). An increase of band area with temperature may be ascribed to a larger contribution of the bands assigned to vibrations for which the change in the dipole moment is higher with temperature, usually asymmetric vibrations. However, to understand the contribution of each vibration (asymmetric and symmetric stretches), absorbance band ratio was obtained and represented as a function of temperature.

In Figure 9, as an example, the temperature dependence of the absorbance band ratio (A_{2923}/A_{2848} ; Asymmetric C-H stretching/Symmetric C-H stretching) for neat PS is presented. The shape of the plot changes significantly compared to that observed in Figure 8 (a). Actually, the A_{2923}/A_{2848} ratio increases with temperature. To explain the continuous increase in band ratio with temperature, we may consider the increase in free volume that provides more space for segmental motions, allowing larger changes in the dipole moment of the vibrations. After the T_g , the increase in free volume is larger, and the

contribution of the changes in the dipole moment is enhanced. In fact, this change in the slope may be attributed to a larger contribution of the change in the dipole moment of the asymmetric C-H stretching vibration, since the change in the dipole moment for the symmetric stretching should remain almost constant with temperature. Consequently, the dipole moment changes more significantly, being the density effect partially hindered.

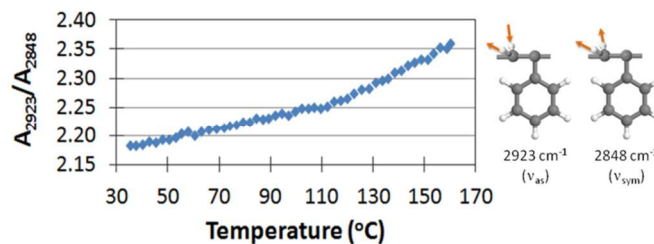


Fig. 9. Temperature dependence of absorbance band ratio (A_{2923}/A_{2848}) for neat PS.

From the analysis of these bands one may conclude that the contribution of the asymmetric band vibrations is enhanced when free volume increases, i.e. after the thermal transition. Other remarkable conclusion is the fact that the thermal transition is detected at lower temperatures when aromatic CH vibrations are considered (110-120°C) compared to that observed using the aliphatic CH vibrations (starting at 120 °C). Other researchers such as I. Noda [43] had also observed two different transition temperatures assigned to the aromatic side groups motions and the dynamics of the whole macromolecule respectively.

Based on our results and continuing with the idea proposed by Noda, the following interpretation can be given to the PS dynamics. As temperature increases, there must be a first separation between the phenyl rings of polystyrene. This process can be considered to occur at a lower temperature range (110-120 °C) what is, in fact, inferred from the analyses of the bands associated to the aromatic CHs. This means that first, it is necessary to overcome the energy necessary to break the specific interactions taking place between the phenyl groups, with a sliding and rotation of the stacking of aromatic rings. After that, the separation of the macromolecules will proceed. This would mean that transition from glassy state to rubbery state must take place in a two-steps process that would consist of the rupture of the specific interactions that take place among the polymer chains followed by the separation and subsequent flow of the macromolecules themselves. This process is schematically shown in the illustrations of Figure 10: (a) At temperatures below 100 °C the PS is in its glassy state where specific interactions between the electron clouds of the aromatic rings are dominant; (b) at temperatures around $T = 110-120$ °C sliding and rotation of the phenyl rings occurs and (c) at temperatures well above 120 °C the backbone of the chains achieves higher mobility allowing polymer conformational changes.

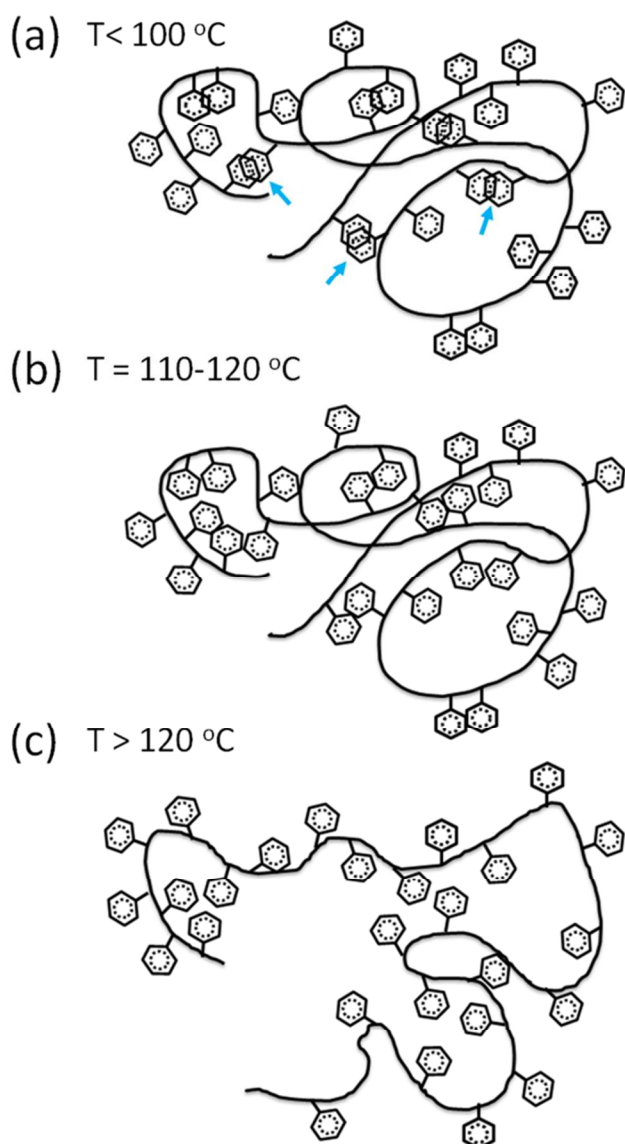


Fig. 10. Illustration of the two-step process associated to the glass transition of PS: (a) Glassy state of the polymer; (b) sliding and rotation of the phenyl rings occurs and (c) higher mobility of the PS backbone with conformational changes.

From a macromolecular point of view, it is generally accepted that the glass transition temperature corresponds to the temperature at which the polymer chains experience segmental motions. Sometimes the glass transition temperature, T_g , is referred to as the temperature at which the activation energy for the cooperative movement of 50 or so units of the polymer chains is exceeded. This allows molecular chains to slide past each other when a force is applied [45]. However, based on the experimental results of the present work, a slightly different perspective of the glass transition process can be proposed. Glass transition temperature may be defined as the temperature at which the polymer acquires the energy necessary to overcome the specific interactions that hold the polymer chains without free motion. For example, in the case of PS, it applies to the inter- and intra-molecular interactions that produce the

stacking of the aromatic rings. Therefore, this fact is indeed of great importance, since intermolecular interactions may modify the physical properties of the whole material which is completely in accordance with W. Xia and S. Ketten who recently stated that intermolecular interactions between polymer chains may be used to tune the T_g of amorphous polymers, thus producing tailor-made polymers with controlled physical or thermal behavior [46].

Conclusions

A new point of view of the dynamics of polystyrene, PS, and PS/BaTiO₃ composites was obtained by an original way of analyzing the FTIR spectra. Results arising from band absorbance and spectral shifts showed that three main regions can be identified in the PS FTIR spectra: i) region I, less sensitive to thermal transitions, assigned to the out-of-plane CH bond vibrations; ii) region II, very sensitive to thermal transitions, assigned to the in-plane vibrations and iii) region III, that corresponds to the stretching vibrations of aromatic and aliphatic C-H bonds which presented the highest changes when a thermal transition occurs.

The vibration frequency or in particular the average wavenumber (first moment), $\langle\nu\rangle$, dependencies with temperature, was explained in terms of i) hot bands and ii) disruption of phenyl oligomers by overcoming specific interactions. Significant findings about the role that these interactions might play on the different kind of bond vibrations were drawn. For vibrations in region II the changes of the π -electron distribution must be higher than for those in region I. The disruption of phenyl-phenyl interactions after the T_g allowed to obtain transition temperatures from the changes in the linearity when plotting $\langle\nu\rangle$ vs T for bands in region II. Changes in the slope of band area with temperature were interpreted in terms of the variation of the change in the dipole moment of the bonds involved in the transition with temperature.

A careful analysis of the aliphatic and aromatic C-H stretching vibrations of PS led us to propose a different approximation to the process of the glass transition temperature of PS based on a two-step process: i) sliding and rotation of the phenyl rings between 110°C and 120°C and ii) PS conformational changes above 120°C. Finally, although the presence of BaTiO₃ particles does not seem to exert any specific effect on the PS dynamics in the glassy state, the Curie transition of these particles might induce a kind of confinement effect observable by FTIR.

Acknowledgements

Authors gratefully acknowledge financial support of the Ministerio de Ciencia e Innovación (MAT2010-16815).

Notes and references

^a Departamento de Ciencia e Ingeniería de Materiales e Ingeniería Química and IQMAAB. Universidad Carlos III de Madrid. Av. Universidad 30, 28911 Leganés (Spain). E-mail: javid@ing.uc3m.es; Tel.: +34 91 624 8870

Electronic Supplementary Information (ESI) available: [details of any supplementary information available should be included here]. See DOI: 10.1039/b000000x/

- 1 M. Böhning, H. Goering, N. Hao, R. Mach, A. Schönhals, *Polym. Adv. Technol.*, 2005, **16**, 262–268.
- 2 P.M. Ajayan, L.S. Schadler, V.P. Braun, *Nanocomposite Science and Technology*, Wiley VCH, New York, 2003.
- 3 S.S. Ray, V. Bousmina, *Polymer Nanocomposites and Their Applications*, American Scientific Publishers, Valencia, CA, 2006.
- 4 J. González-Benito, E. Castillo, J.F. Caldito, *Eur. Polym. J.*, 2013, **49**, 1747–1752.
- 5 P.D. Castrillo, D. Olmos, D.R. Amador, J. Gonzalez-Benito, *J. Colloid Interface Sci.*, 2007, **308**, 318–324.
- 6 P.D. Castrillo, D. Olmos, J. Gonzalez-Benito. *J. Appl. Polym. Sci.* 2008, **111**, 2062–2072.
- 7 J. Gonzalez-Benito, G. Gonzalez-Gaitano, *Macromolecules*, 2008, **41**, 4777–4785.
- 8 D. Olmos, C. Domínguez, P.D. Castrillo, J. González- Benito, *Polymer*, 2009, **50**, 1732–1742.
- 9 J. Gonzalez-Benito, D. Olmos. Efficient dispersion of nanoparticles in thermoplastic polymers. *Plastics Research Online* (2010oi:10.1002/spepro.002566).
- 10 D. Olmos, E. Rodríguez-Gutierrez, J. González-Benito, *Polym Composites*, 2012, **33**, 2009–2021.
- 11 C. G. Robertson, C.J. Lin, M. Rackaitis, C.M. Roland, *Macromolecules*, 2008, **41**, 2727–2731.
- 12 P. Rittigstein, R.D. Priestley, L.J. Broadbelt, J.M. Torkelson, *Nature Materials* 2007, **6**, 278–282.
- 13 X. Y. Tian, X. Zhang, W.T. Liu, J. Zheng, C.J. Ruan, P. J. Cui, *Macromol. Sci., Phys.* 2006, **45**, 507–513.
- 14 V. Krikorian, D. Pochan, *Chem. Mater.* 2003, **15**, 4317–4324.
- 15 R. B. Bogoslovov, C.M. Roland, A.R. Ellis, A. M. Randall, C. G. Robertson, *Macromolecules*, 2008, **41**, 1289–1296.
- 16 J.L. Koenig, *Spectroscopy of Polymers*. Elsevier, New York, 1999.
- 17 Z. Chen, J.N. Hay, M.J. Jenkins, *Thermochim Acta*, 2013, **552**, 123–130.
- 18 B.J. Holland, J.N. Hay, *Polymer*, 2001, **42**, 4825–4835.
- 19 B.J. Holland, J.N. Hay, *Polymer*, 2002, **43**, 1835–1847.
- 20 S.V. Levchik, L. Costa, G. Camino, *Polym. Degrad. Stab.*, 1993, **43**, 43–54.
- 21 B.J. Holland, J.N. Hay, *Polymer*, 2001, **42**, 6775–6783.
- 22 Z. Chen, J.N. Hay, M.J. Jenkins, *Eur. Polym. J.*, 2012, **48**, 1586–1610.
- 23 S. Watanabe, I. Noda, Y. Ozaki, *Polymer* 2008, **49**, 774–784.
- 24 H. Shinzawaa, M. Nishida, T. Tanaka, W. Kanematsu, W. *Vibr. Spectros.*, 2012, **60**, 50–53.
- 25 P. Painter, M. Sobkowiak, Y. Park, *Macromolecules*, 2007, **40**, 1730–1737.
- 26 P. Painter, M. Sobkowiak, Y. Park, *Macromolecules*, 2007, **40**, 1738–1745.
- 27 X. Liang, D. Huang, *J. Macromol. Sci., Part B: Physics*, 2012, **51**, 348–357.
- 28 D.Olmos, J. González-Benito, *Colloid Polym. Sci.*, 2006, **284**, 654–667.
- 29 S. G. Turrión, D. Olmos, N. Ekizoglou, J. González-Benito, *Polymer*, 2005, **46**, 4023–4031.
- 30 R. L. Morón, D. Olmos, J. González-Benito, *Compos. Sci. Technol.*, 2006, **66**, 2758–2768.
- 31 D. Olmos, A. García-López, J. González-Benito, *Mater. Lett.*, 2013, **97**, 8–10.
- 32 D. Olmos, J.M. Martínez-Tarifa, G. González-Gaitano, J. González-Benito, *Polym. Testing*, 2012, **31**, 1121–1130.
- 33 C.Y. Liang, S. Krimm, *J. Mol. Spectrosc.*, 1959, **3**, 554–574.
- 34 G. Chen, S. Liu, S. Chen, Z. Qi. *Macromolecular Chem. Phys.*, 2001, **202**, 1189–1193.
- 35 F.J. Torres, B. Civalleri, C. Pisani, P. Musto, A.R. Albuñia, G. Guerra, *J. Phys. Chem. B*, 2007, **111**, 6327–6335.
- 36 F.J. Torres, B. Civalleri, A. Meyer, P. Musto, A.R. Albuñia, P. Rizzo, G. Guerra, *J. Phys. Chem. B*, 2009, **113**, 5059–5071.
- 37 P. Pan, B. Zhu, T. Dong, K. Yazawa, T. Shimizu, T. Masataka, Y. Inoue, *J. Chem. Phys.*, 2008, **129**, 184902.
- 38 L. D’Ilario, M. Lucarini, A. Martinelli, A. Piozzi, *Eur. Polym. J.* 1997, **33**, 1809–1811.
- 39 Y. Zhang, J. Zhang, Y. Lu, Y. Duan, S. Yan, D. Shen, *Macromolecules*, 2004, **37**, 2532–2537.
- 40 P. Papadopoulos, W. Kossack, F. Kremer, *Soft Matter*, 2013, **9**, 1600–1603.
- 41 F. Mikes, J. González-Benito, B. Serrano, J. Bravo, J. Baselga, *Polymer*, 2002, **43**, 4331–4339.
- 42 J. Coates. *Interpretation of Infrared Spectra, A Practical Approach in Encyclopedia of Analytical Chemistry*. R.A. Meyers (Ed.) pp. 10815 – 10837. John Wiley & Sons Ltd, Chichester, 2000.
- 43 I. Noda, A.E. Dowrey, C. Marcott, *Vibrational Spectroscopy*, 2009, **51**, 22–27.
- 44 A. Anton, *Detection of polymer transition temperatures by infrared absorption spectrometry. J. Appl. Polym. Sci.*, 1968, **12**, 2117–2128.
- 45 J. M. G. Cowie, V. Arrighi, *Polymers: Chemistry and Physics of Modern Materials*, 3rd Edn. (CRC Press, 2007) ISBN 0748740732.
- 46 W. Xia, S. Keten, *Langmuir*, 2013, **29**, 12730–12736.